Supporting Information

Revealing the Structure-Activity Relationship in Woven Covalent Organic Frameworks for Electrocatalytic Oxygen Reduction Reaction

*Jiawen Li, Peng Liu, Jianxin Mao, Jianyue Yan, and Wenbo Song**

College of Chemistry, Jilin University, Changchun 130012, P.R. China.

**E-mail: wbsong@jlu.edu.cn*

Contents

1. Lattice parameters

Table S1. Pawley-refined lattice parameters of COF-112

Lattice parameters	COF-112Co	COF-112Fe
a (Å)	19.7833	19.8969
b (Å)	25.1229	23.4190
c (Å)	11.8086	12.8494
α (°)	90	90
β (°)	90	90
γ (°)	90	90

2. TEM images

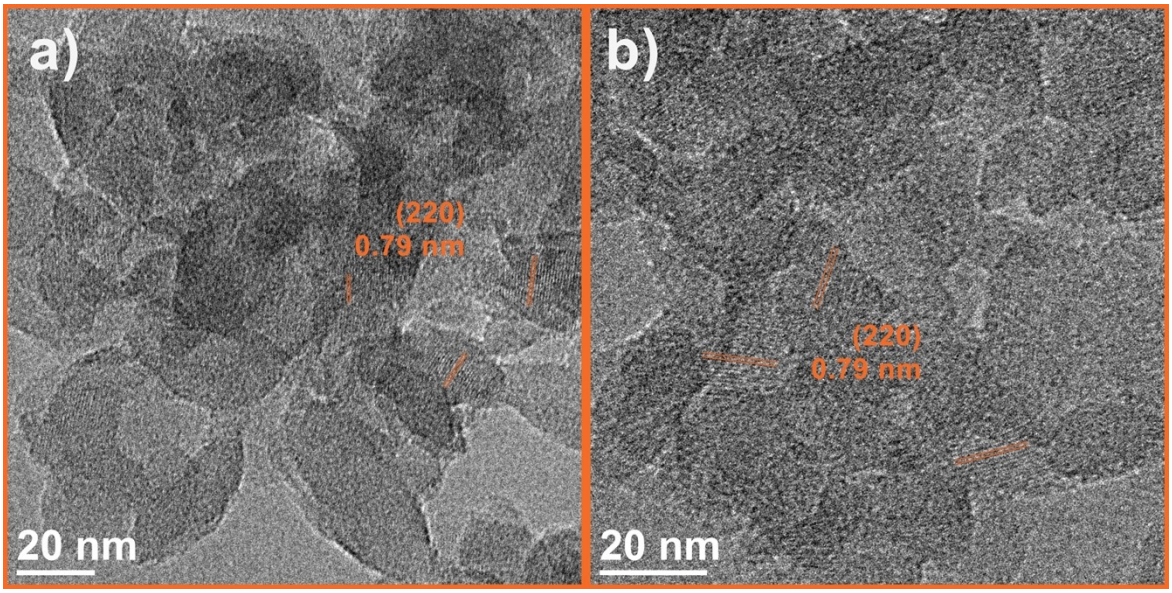

Figure S1. TEM images of **COF-112Co** (a, b).

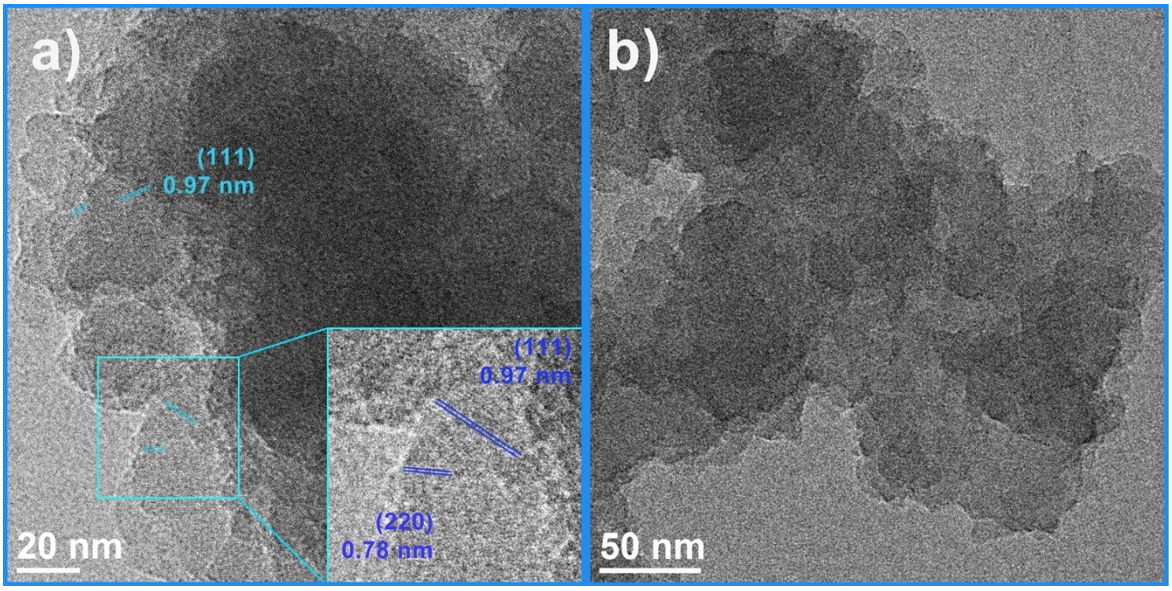

Figure S2. TEM images of **COF-112Fe** (a, b).

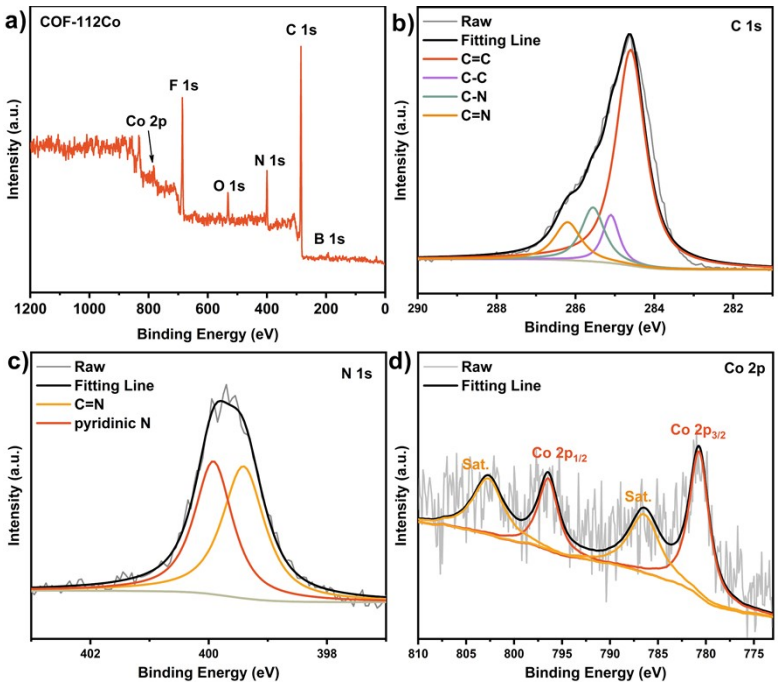

Figure S3. XPS spectra of **COF-112Co**: a) survey, b) C 1s, c) N 1s, d) Co 2p.

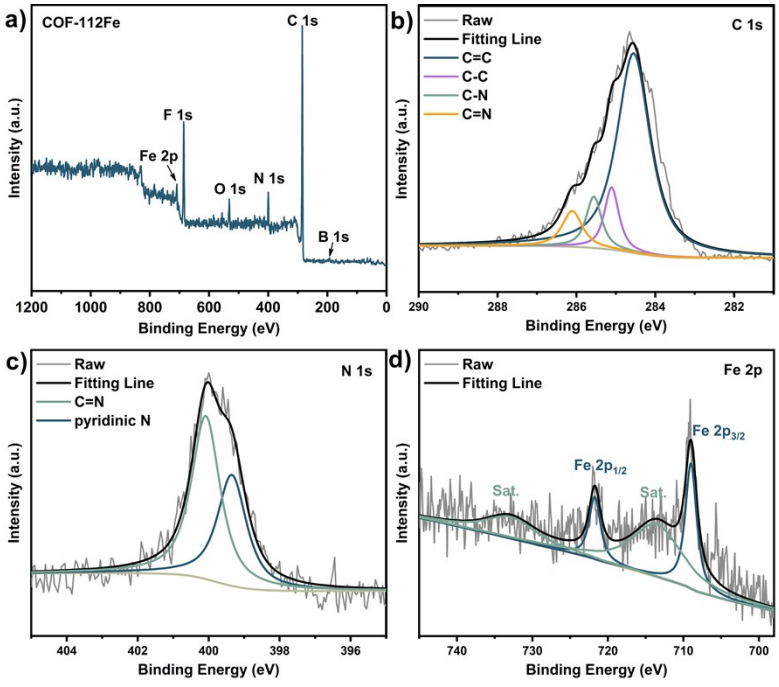

Figure S4. XPS spectra of **COF-112Fe**: a) survey, b) C 1s, c) N 1s, d) Fe 2p.

3. XPS spectra

Table S2. Element content analysis calculated from XPS.

COFs	Co (at%)	Fe (at%)	B (at%)	C (at%)	N (at%)	F (at%)
COF-112Co	1.73	-	7.89	66.83	10.13	13.42
COF-112Fe	-	3.30	5.91	70.94	8.80	11.06

4. Electrocatalytic Analysis

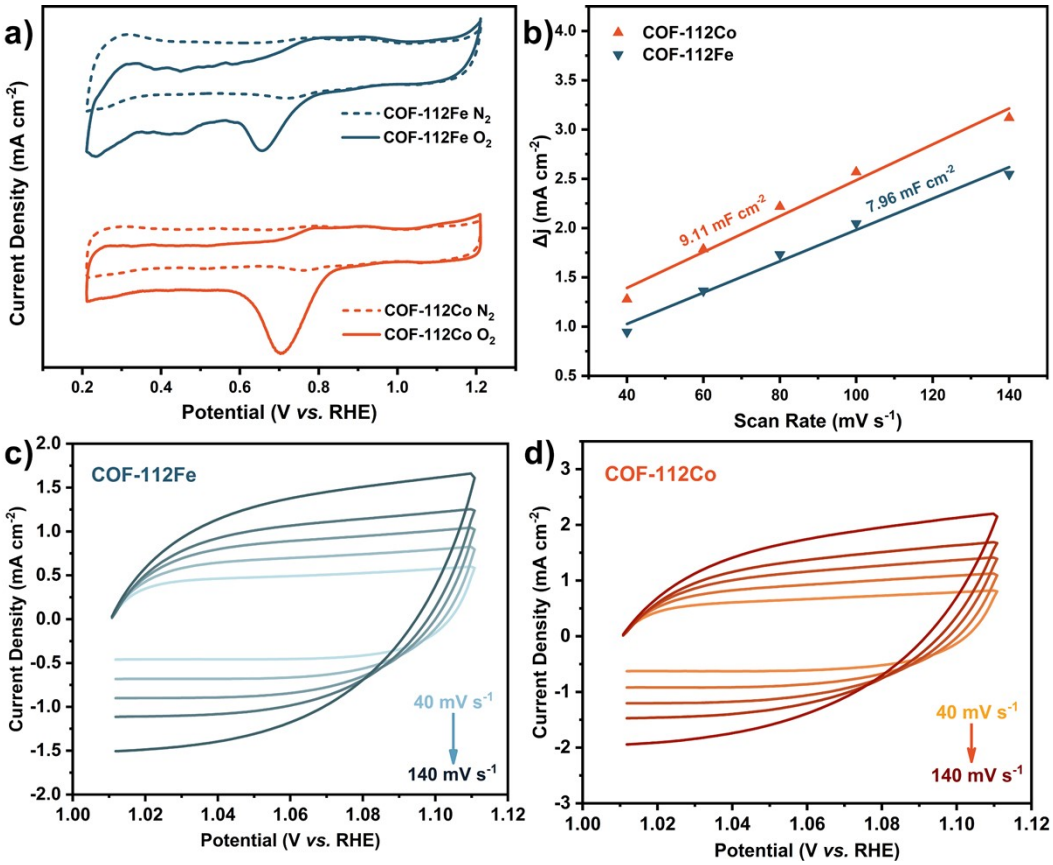

Figure S5. (a) CVs curves of **COF-112Co** and **COF-112Fe** in O_2 (solid line) or N_2 (dashed line) -saturated 0.1M KOH. (b) Scan rate dependent-current densities at 1.06 V vs. RHE. CVs in non-faradaic region of **COF-112Fe** (c) and **COF-112Co** (d).

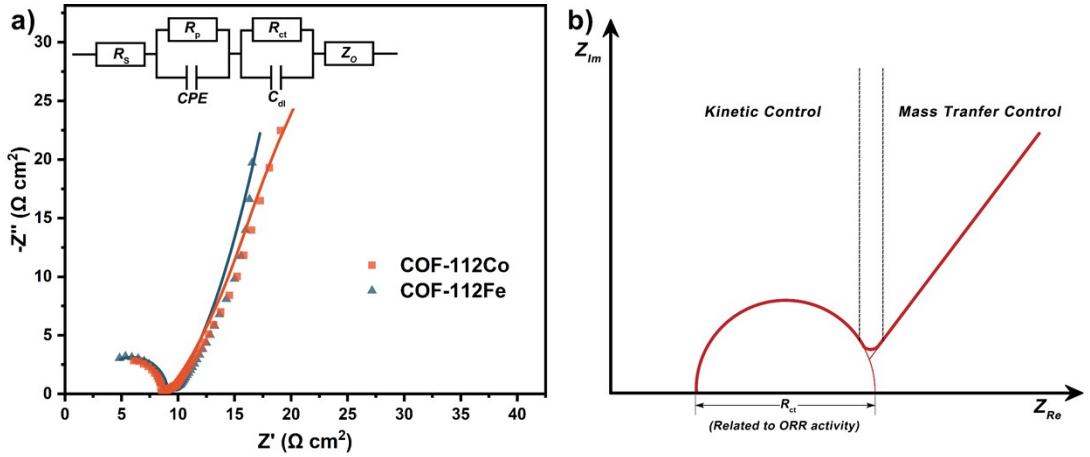

Figure S6. (a) Nyquist plots for **COF-112Co** and **COF-112Fe**, (b) The relation between ORR process and EIS.

In the Nyquist plots, the charge-transfer resistance (R_{ct}) is the main parameter that reflects the ORR activity. In contrast, the linear part of EIS spectra is controlled by diffusion (mass transfer), which is not the main parameter that influences the ORR intrinsic activity (Figure S6b). The R_{ct} of COF-112Co (5.50 Ω cm^2) is smaller than that of COF-112Fe (6.26 Ω cm^2), indicating the faster ORR kinetics of COF-112Co.

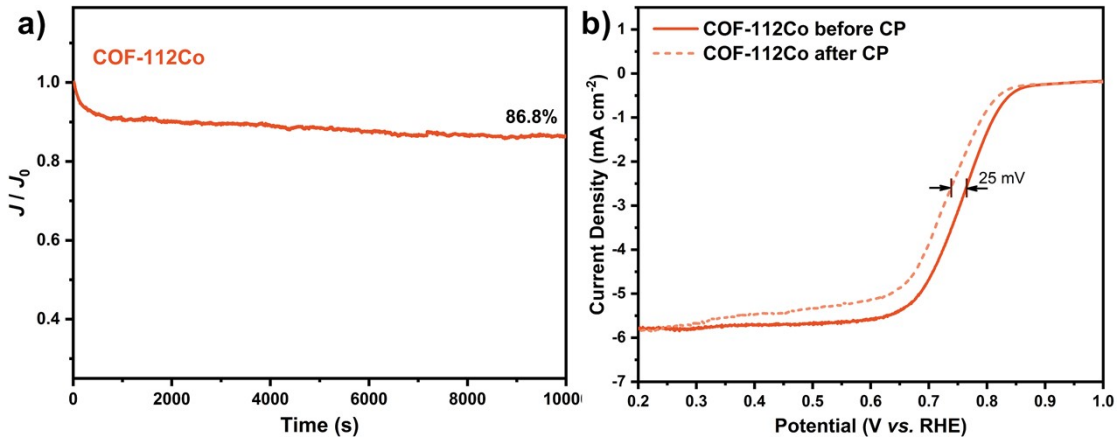

Figure S7. (a) Chronoamperometry test at 0.6 V *vs.* RHE of **COF-112Co**, (b) LSV plots (at 1600 rpm) of **COF-112Co** before and after chronoamperometry.

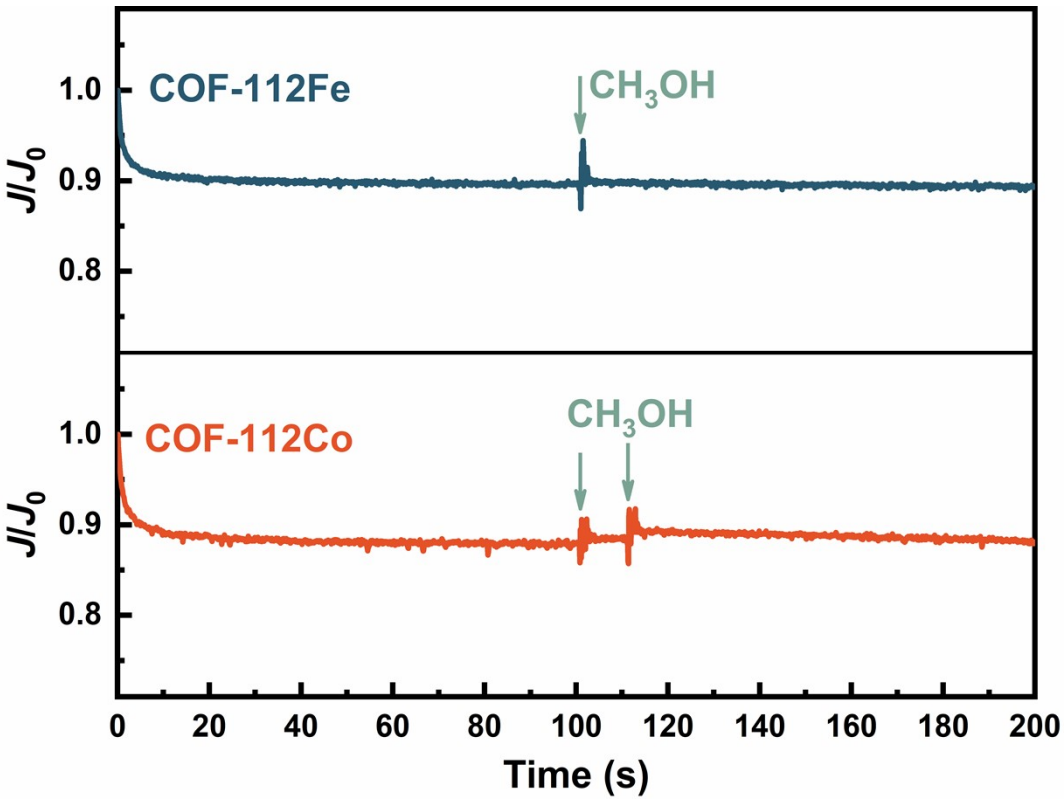

Figure S8. Methanol crossover tests of COF-112Co and COF-112Fe.

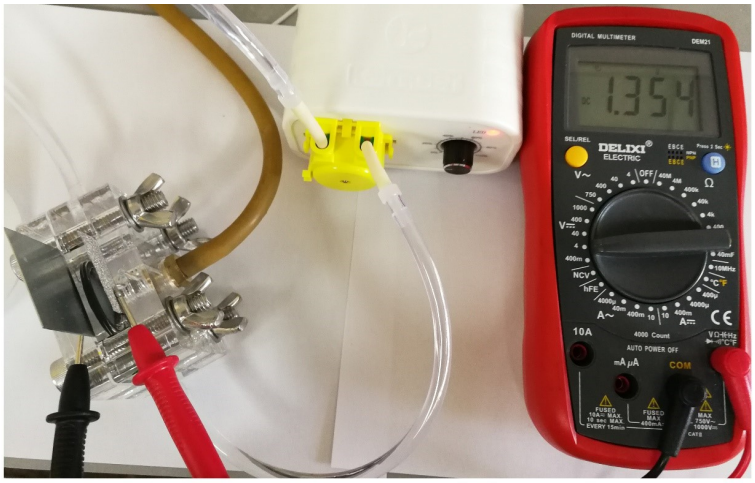

Figure S9. Open-circuit voltage of the Zn-air battery of **COF-112Co**.

5. Theoretical Computation Section

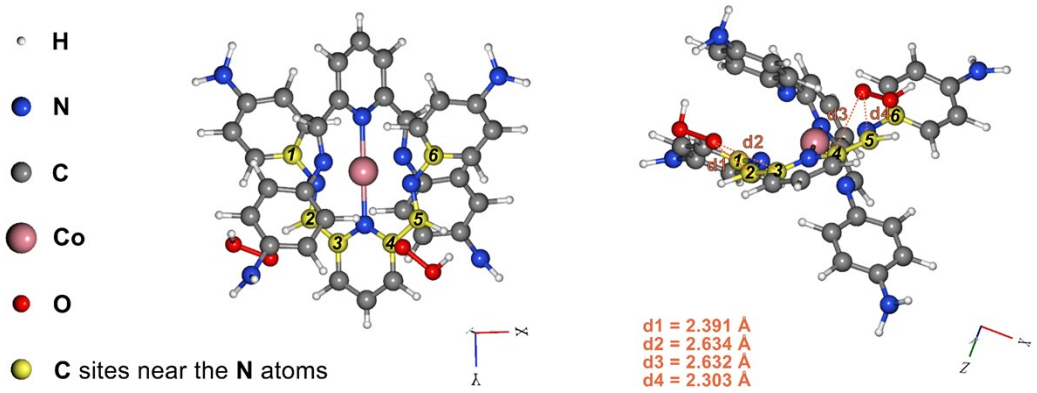

Figure S10. DFT calculation model of **COF-112Co**.

Table S3. DFT adsorption free energies of the ORR intermediates ($*O_2$, *OOH, *O, and *OH) for the calculation model of COF-112. ORR limiting potentials and the rate-determine step (RDS) are displayed for each row.

Central Metal	Binding Site	ΔG*OO (eV)	ΔG*OOH (eV)	ΔG*O (eV)	ΔG*OH (eV)	Limiting Barrier (eV)	Rate-determine Step
Co	C2&C3	4.561	4.325	3.103	1.343	0.994	$*O_2 \rightarrow *OOH$
Co	C4&C5	4.599	4.274	2.984	1.177	0.904	$*O_2 \rightarrow *OOH$
Fe	C4&C5	4.550	4.247	3.002	1.143	0.927	$*O_2 \rightarrow *OOH$

6. Linkage Conversion Section

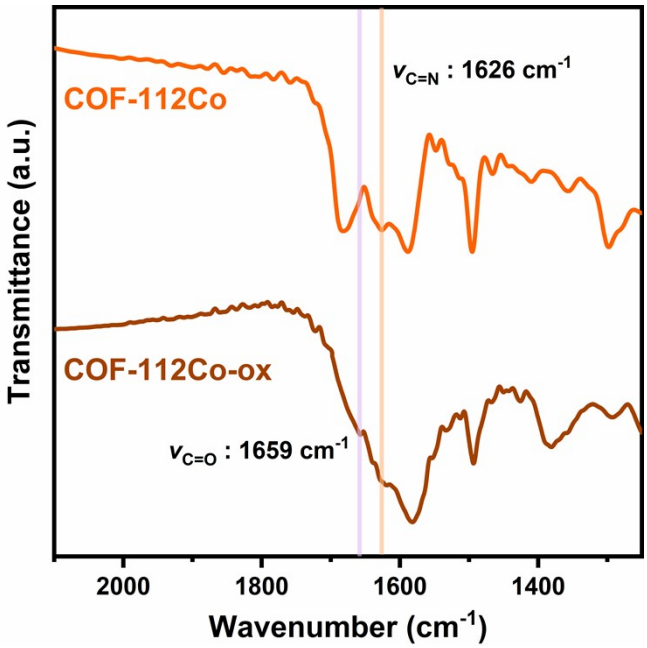

Figure S11. FT-IR spectra of **COF-112Co** and **COF-112Co-ox**.

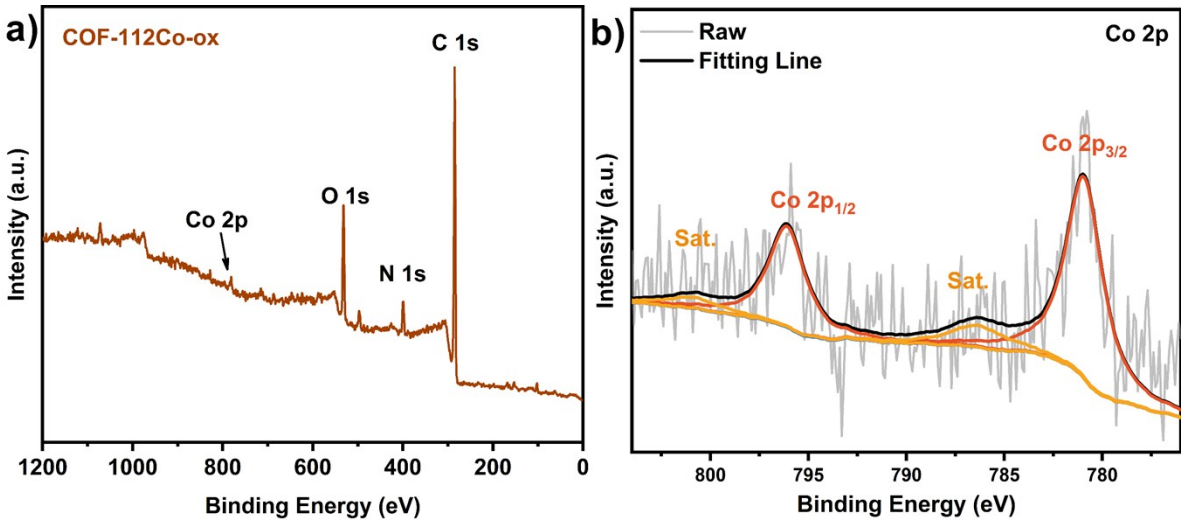

Figure S12. XPS spectra of **COF-112Co-ox**: a) survey, b) Co 2p.

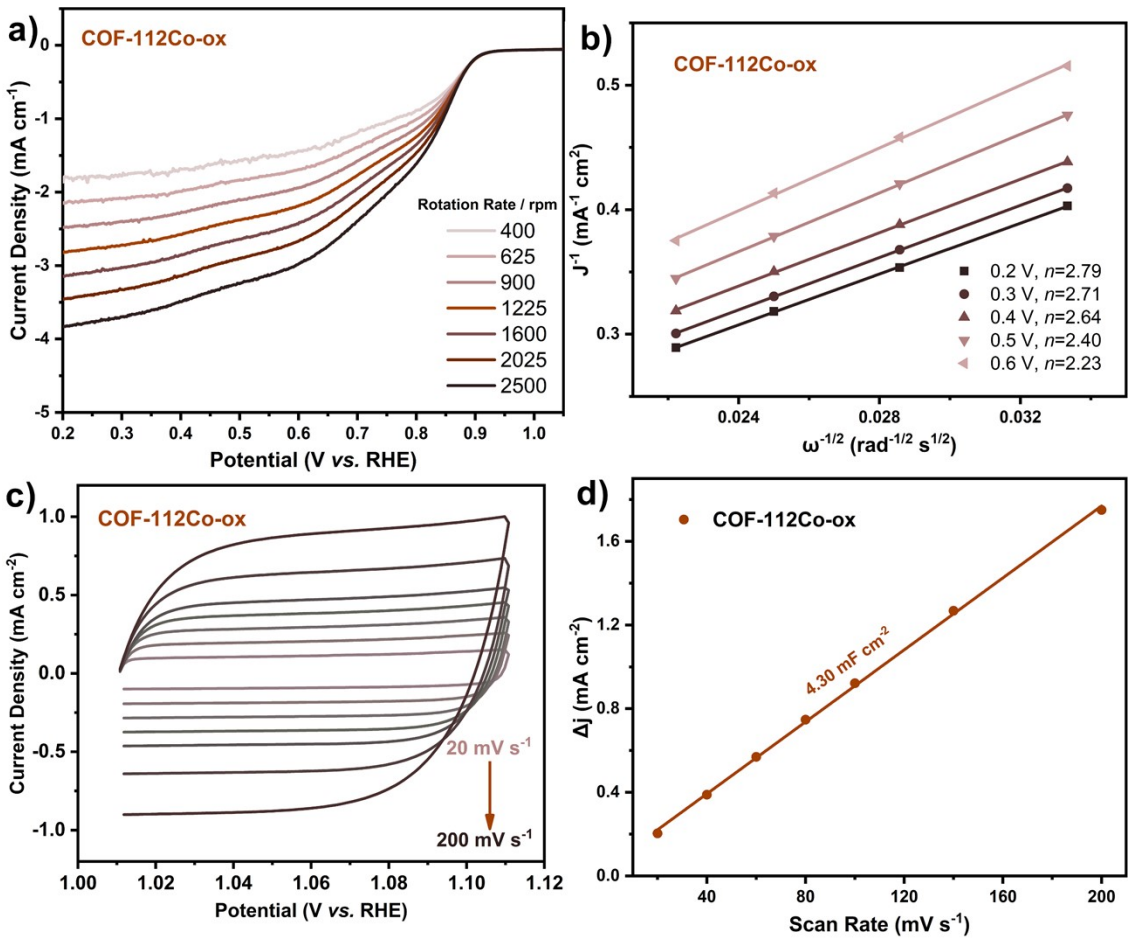

Figure S13. a) RDE plots, b) K-L plots, c) CV curves in non-faradic region, and d) Scan rate dependent-current densities at 1.06 V vs. RHE. of **COF-112Co-ox**.

The electron transfer numbers calculated from RDE measurements are 2.23~2.64 (0.6V~0.4 V vs. RHE), similar to the results of RRDE.

7. Comparison Table

Table S4. Comparisons of the ORR activity of pristine POP catalysts.

Catalyst	Electrolyte	Half-wave Potential (V *vs.* RHE)	Current Density (mA cm^{-2}) @E (V *vs.* RHE)	Electron transfer number @E (V *vs.* RHE)	Rotate speed (rpm)	Ref.
COF-112Co	**0.1M KOH**	**0.76**	**5.78@0.2**	**3.86@0.2**	**1600**	**This work**
NDI-CON	0.1M NaOH	~0.68	~3.72@0.3	3.6	1500	1
Co@TPA−PDI	0.1M KOH	~0.71	5.7@0.3	3.9	1600	2
PTM-CORF	0.1M KOH	~0.69	~5.7@0.17	3.89@0.6	1600	3
COF_{BTC}	0.1M KOH	0.91	~5.3@0.2	3.95@0.85	1600	4
CoCOF-Py-rGO	0.1M KOH	0.76	4.72@0.2	3.7@0.2	1600	5
COP/rGO	0.1M KOH	~0.72	~4.31@0.2	3.7@0.75	1600	6
TAPA-PG	0.1M KOH	~0.57	~4.16@0.2	3.84@0.3	1600	7
Co@TAPA-PG	0.1M KOH	~0.63	~4.8@0.2	3.63	1600	7
JUC-528	0.1M KOH	0.70	~5.0@0.2	3.81@0.2	1600	8
G@POF-Co	0.1M KOH	0.81	~5.43@0.2	3.8	1600	9

All of these parameters with "~" are obtained by the graph of LSV curves at 1600 rpm.

References:

1. S. Royuela, E. Martinez-Perinan, M. P. Arrieta, J. I. Martinez, M. M. Ramos, F. Zamora, E. Lorenzo and J. L. Segura, *Chem. Commun.*, 2020, **56**, 1267-1270.
2. S. Bhattacharyya, D. Samanta, S. Roy, V. P. Haveri Radhakantha and T. K. Maji, *ACS Appl. Mater. Interfaces*, 2019, **11**, 5455-5461.
3. S. Wu, M. Li, H. Phan, D. Wang, T. S. Herng, J. Ding, Z. Lu and J. Wu, *Angew. Chem. Int. Ed.*, 2018, **57**, 8007-8011.
4. P. Peng, L. Shi, F. Huo, C. Mi, X. Wu, S. Zhang and Z. Xiang, *Sci. Adv.*, 2019, **5**, eaaw2322.
5. Q. Zuo, G. Cheng and W. Luo, *Dalton Trans.*, 2017, **46**, 9344-9348.
6. J. Guo, C. Y. Lin, Z. Xia and Z. Xiang, *Angew. Chem. Int. Ed.*, 2018, **57**, 12567-12572.
7. A. Singh, D. Samanta and T. K. Maji, *ChemElectroChem*, 2019, **6**, 3756-3763.
8. D. Li, C. Li, L. Zhang, H. Li, L. Zhu, D. Yang, Q. Fang, S. Qiu and X. Yao, *J. Am. Chem. Soc.*, 2020, **142**, 8104-8108.
9. B. Q. Li, S. Y. Zhang, X. Chen, C. Y. Chen, Z. J. Xia and Q. Zhang, *Adv. Funct. Mater.*, 2019, **29**, 1901301.